

Isolated sub-fs XUV pulse generation in Mn plasma ablation

R. A. Ganeev,^{1,2,3,*} T. Witting,¹ C. Hutchison,¹ F. Frank,¹ M. Tudorovskaya,⁴
M. Lein,⁴ W. A. Okell,¹ A. Zair,¹ J. P. Marangos,¹ and J. W. G. Tisch¹

¹Blackett Laboratory, Imperial College London, Prince Consort Road, London SW7 2AZ, UK

²Institute of Ion, Plasma, and Laser Technologies, 33, Dormon Yoli Street, Tashkent 100125, Uzbekistan

³Voronezh State University, Voronezh 394006, Russia

⁴Institut für Theoretische Physik and Centre for Quantum Engineering and Space-Time Research (QUEST), Leibniz Universität Hannover, Appelstraße 2, 30167 Hannover, Germany

*r.ganeev@imperial.ac.uk

Abstract: We report studies of high-order harmonic generation in laser-produced manganese plasmas using sub-4-fs drive laser pulses. The measured spectra exhibit resonant enhancement of a small spectral region of about 2.5 eV width around the 31st harmonic (~50eV). The intensity contrast relative to the directly adjacent harmonics exceeds one order of magnitude. This finding is in sharp contrast to the results reported previously for multi-cycle laser pulses [Physical Review A 76, 023831 (2007)]. Theoretical modelling suggests that the enhanced harmonic emission forms an isolated sub-femtosecond pulse.

©2012 Optical Society of America

OCIS codes: (190.4160) Multiharmonic generation; (190.2620) Harmonic generation and mixing.

References and links

1. A. McPherson, G. Gibson, H. Jara, U. Johann, T. S. Luk, I. A. McIntyre, K. Boyer, and C. K. Rhodes, "Studies of multiphoton production of vacuum-ultraviolet radiation in the rare gases," *J. Opt. Soc. Am. B* **4**(4), 595–601 (1987).
2. P. B. Corkum, "Plasma perspective on strong field multiphoton ionization," *Phys. Rev. Lett.* **71**(13), 1994–1997 (1993).
3. Y. Liang, S. Augst, S. L. Chin, Y. Beaudoin, and M. Chaker, "High harmonic generation in atomic and diatomic molecular gases using intense picosecond laser pulses—a comparison," *J. Phys. B* **27**(20), 5119–5130 (1994).
4. A. Flettner, T. Pfeifer, D. Walter, C. Winterfeldt, C. Spielmann, and G. Gerber, "High-harmonic generation and plasma radiation from water microdroplets," *Appl. Phys. B* **77**(8), 747–751 (2003).
5. S. Ghimire, A. D. DiChiara, E. Sistrunk, P. Agostini, L. F. DiMauro, and D. A. Reis, "Observation of high-order harmonic generation in a bulk crystal," *Nat. Phys.* **7**(2), 138–141 (2011).
6. R. A. Ganeev, "Generation of high-order harmonics of high-power lasers in plasmas produced under irradiation of solid target surfaces by a prepulse," *Phys. Usp.* **52**(1), 55–77 (2009).
7. H. Kjeldsen, F. Folkmann, B. Kristensen, J. B. West, and J. E. Hansen, "Absolute cross section for photoionization of Mn⁺ in the 3p region," *J. Phys. B* **37**(6), 1321–1330 (2004).
8. G. V. Marr and J. B. West, "Absolute photoionization cross-section tables for helium, neon, argon, and krypton in the VUV spectral regions," *At. Data Nucl. Data Tables* **18**(5), 497–508 (1976).
9. J. Levesque, D. Zeidler, J. P. Marangos, P. B. Corkum, and D. M. Villeneuve, "High harmonic generation and the role of atomic orbital wave functions," *Phys. Rev. Lett.* **98**(18), 183903 (2007).
10. A. D. Shiner, B. E. Schmidt, C. Trallero-Herrero, H. J. Wörner, S. Patchkovskii, P. B. Corkum, J.-C. Kieffer, F. Légaré, and D. M. Villeneuve, "Probing collective multi-electron dynamics in xenon with high-harmonic spectroscopy," *Nat. Phys.* **7**(6), 464–467 (2011).
11. R. A. Ganeev, M. Suzuki, M. Baba, H. Kuroda, and T. Ozaki, "Strong resonance enhancement of a single harmonic generated in the extreme ultraviolet range," *Opt. Lett.* **31**(11), 1699–1701 (2006).
12. R. A. Ganeev, P. A. Naik, H. Singhal, J. A. Chakera, and P. D. Gupta, "Strong enhancement and extinction of single harmonic intensity in the mid- and end-plateau regions of the high harmonics generated in weakly excited laser plasmas," *Opt. Lett.* **32**(1), 65–67 (2007).
13. R. Ganeev, L. Bom, J.-C. Kieffer, M. Suzuki, H. Kuroda, and T. Ozaki, "Demonstration of the 101st harmonic generated from laser-produced manganese plasma," *Phys. Rev. A* **76**(2), 023831 (2007).
14. R. A. Ganeev, M. Suzuki, M. Baba, and H. Kuroda, "Extended high-order harmonics from laser-produced Cd and Cr plasmas," *Appl. Phys. Lett.* **94**(5), 051101 (2009).
15. M. Hentschel, R. Kienberger, C. Spielmann, G. A. Reider, N. Milosevic, T. Brabec, P. B. Corkum, U. Heinzmann, M. Drescher, and F. Krausz, "Attosecond metrology," *Nature* **414**(6863), 509–513 (2001).

16. T. Witting, F. Frank, W. A. Okell, C. A. Arrell, J. P. Marangos, and J. W. G. Tisch, "Sub-4-fs laser pulse characterization by spatially resolved spectral shearing interferometry and attosecond streaking," *J. Phys. B* **45**(7), 074014 (2012).
17. C. Altucci, J. W. G. Tisch, and R. Velotta, "Single attosecond light pulses from multi-cycle laser sources," *J. Mod. Opt.* **58**(18), 1585–1610 (2011).
18. J. S. Robinson, C. A. Haworth, H. Teng, R. A. Smith, J. P. Marangos, and J. W. G. Tisch, "The generation of intense, transform-limited laser pulses with tunable duration from 6 to 30 fs in a differentially pumped hollow fibre," *Appl. Phys. B* **85**(4), 525–529 (2006).
19. T. Witting, F. Frank, C. A. Arrell, W. A. Okell, J. P. Marangos, and J. W. G. Tisch, "Characterization of high-intensity sub-4-fs laser pulses using spatially encoded spectral shearing interferometry," *Opt. Lett.* **36**(9), 1680–1682 (2011).
20. R. A. Ganeev, T. Witting, C. Hutchison, F. Frank, P. V. Redkin, W. A. Okell, D. Y. Lei, T. Roschuk, S. A. Maier, J. P. Marangos, and J. W. G. Tisch, "Enhanced high-order harmonic generation in a carbon ablation plume," *Phys. Rev. A* **85**(1), 015807 (2012).
21. D. Kilbane, E. T. Kennedy, J.-P. Mosnier, P. Kampen, and J. T. Costello, "On the 3p-subshell photoabsorption spectra of iron-group ions: the case of Mn^{2+} ," *J. Phys. B* **38**(1), L1–L8 (2005).
22. V. K. Dolmatov, "Characteristic features of the 3p absorption spectra of free iron-group elements due to the duplicity of the 'inner-valence' 3d electrons. Application to Mn^{2+} ," *J. Phys. B* **29**(19), L687–L692 (1996).
23. J. B. West, J. E. Hansen, B. Kristensen, F. Folkmann, and H. Kjeldsen, "Revised interpretation of the photoionization of Cr^+ in the 3p excitation region," *J. Phys. B* **36**(19), L327–L333 (2003).
24. V. Strelkov, "Role of autoionizing state in resonant high-order harmonic generation and attosecond pulse production," *Phys. Rev. Lett.* **104**(12), 123901 (2010).
25. D. B. Milošević, "Resonant high-order harmonic generation from plasma ablation: Laser intensity dependence of the harmonic intensity and phase," *Phys. Rev. A* **81**(2), 023802 (2010).
26. M. V. Frolov, N. L. Manakov, and A. F. Starace, "Potential barrier effects in high-order harmonic generation by transition-metal ions," *Phys. Rev. A* **82**(2), 023424 (2010).
27. P. V. Redkin and R. A. Ganeev, "Simulation of resonant high-order harmonic generation in three-dimensional fullerene-like system by means of multiconfigurational time-dependent Hartree-Fock approach," *Phys. Rev. A* **81**(6), 063825 (2010).
28. M. Tudorovskaya and M. Lein, "High-order harmonic generation in the presence of a resonance," *Phys. Rev. A* **84**(1), 013430 (2011).
29. M. D. Feit, J. A. Fleck, Jr., and A. Steiger, "Solution of the Schrödinger equation by a spectral method," *J. Comput. Phys.* **47**(3), 412–433 (1982).
30. C. D. Lin, A.-T. Le, Z. Chen, T. Morishita, and R. Lucchese, "Strong-field rescattering physics—self-imaging of a molecule by its own electrons," *J. Phys. B* **43**(12), 122001 (2010).
31. D. B. Milošević, "Theoretical analysis of high-order harmonic generation from a coherent superposition of states," *J. Opt. Soc. Am. B* **23**(2), 308–317 (2006).
32. D. Gabor, "Theory of communication. Part I: The analysis of information," *J. Inst. Electr. Eng.* **93**, 429–441 (1946).
33. L. E. Chipperfield, L. N. Gaier, P. L. Knight, J. P. Marangos, and J. W. G. Tisch, "Conditions for the reliable production of attosecond pulses using ultra-short laser-generated high harmonics," *J. Mod. Opt.* **52**(2–3), 243–260 (2005).
34. E. Goulielmakis, M. Schultze, M. Hofstetter, V. S. Yakovlev, J. Gagnon, M. Uiberacker, A. L. Aquila, E. M. Gullikson, D. T. Attwood, R. Kienberger, F. Krausz, and U. Kleineberg, "Single-cycle nonlinear optics," *Science* **320**(5883), 1614–1617 (2008).

1. Introduction

The interaction of atoms with strong laser pulses causes the emission of coherent high-frequency photons in the extreme ultraviolet (XUV) spectral range [1]. This process is known as high-order harmonic generation (HHG). HHG from gas-phase targets is usually explained in terms of the classical three-step recollision model [2], in which an electron wavepacket is launched into the continuum and accelerated by the strong electric field of the drive laser pulse before eventually recombining with the parent ion leading to the emission of an XUV photon. In the course of the ongoing efforts to enhance the low XUV harmonic intensities and to study fundamental aspects of HHG, alternative media such as molecules [3], microdroplets [4], and solids [5] have been employed.

The present work focuses on HHG from transition metal plasmas [6]. These are very promising targets in view of the giant resonances found in the photoionization cross sections. For example, the Mn^+ cross section is ~ 40 Mb at 50 eV photon energy [7], whereas rare gas atoms have cross sections between 1 and 8 Mb at this photon energy [8]. Photorecombination - the third step in the recollision model - is the inverse process of photoionization [9] and therefore HHG and photoionization must exhibit the same resonances. This has been

confirmed not only by previous resonance-induced experiments with laser-produced transition metal plasmas but also in a recent study of HHG from xenon gas [10].

Resonance-induced enhancement of a single harmonic or, in some cases, a group of harmonics of the laser radiation allowed considerable improvement of harmonic efficiency in some specific XUV spectral ranges related with high oscillator strengths of ionic states of metals. This was confirmed in multiple studies following the initial observation of this phenomenon in indium plasma [11]. In particular, the strong enhancement of a single harmonic was reported in Cr [12], and Mn [13] plasmas. The Mn plasma is of special interest since it shows the highest harmonic cut-off energy observed in plasma plumes (101st harmonic [13]). In previous studies multi-cycle (30 [13] and 140 fs [14]) laser pulses were employed and the generation of all harmonics in the plateau was observed together with a strongly enhanced single harmonic.

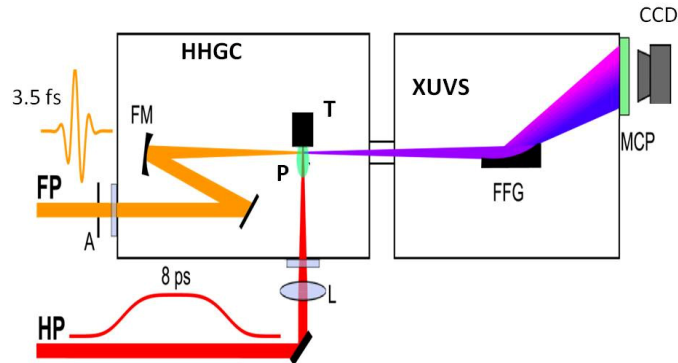


Fig. 1. Experimental setup for harmonic generation in plasma plumes. FP: femtosecond harmonic drive pulse, HP: picosecond heating pulse, A: aperture, HHGC: high-order harmonic generation chamber, FM: focussing mirror, L: focussing lens, T: target, P: plasma, XUVS: extreme ultraviolet spectrometer, FFG: flat field grating, MCP: microchannel plate and phosphor screen detector, CCD: CCD camera.

Recent progress in the generation of few-cycle pulses allowed the observation of various new effects including the realisation of isolated attosecond-pulse generation in gas media [15–17]. In this connection it is interesting to analyse resonance-induced processes observed in an ablation plume using the shortest available drive laser pulses. In this paper, we present the observation of resonance enhancement in manganese plasmas using sub-4-fs pulses. The most interesting feature observed in these experiments was the suppression of almost all neighbouring harmonics in the vicinity of a resonantly enhanced small spectral range of about 2.5 eV bandwidth covering only a single harmonic at the photon energy of ~ 50 eV. We report HHG studies in Mn plasma at various pulse durations of the drive laser pulse (3.5–25 fs) and compare these results with those obtained using 40 fs pulses. Theoretical modelling suggests that the resonantly enhanced harmonic emission constitutes a near isolated sub-femtosecond pulse. We also analyse the influence of carrier envelope phase on the harmonics from manganese plasma and show some CEP-dependent pictures of Mn HHG spectra.

2. Experimental setup

Our Ti:sapphire laser (Femtolasers Produktions GmbH) provided pulses of 25 fs duration and energies of up to 0.8 mJ at a repetition rate of 1 kHz. These pulses were focused into a 1-m-long differentially pumped hollow core fiber [18] (250 μm inner core diameter) filled with neon. The spectrally broadened pulses at the output of the fiber system were compressed by 10 bounces of double-angle technology chirped mirrors (Ultrafast Innovations GmbH). A pair of fused silica wedges was used to fine tune the pulse compression. High-intensity few-cycle pulses (780 nm central wavelength, 0.2 mJ, 3.5 fs) were typically obtained in this system. The compressed pulses were characterized spatially and temporally to high precision with spatially

encoded arrangement for spectral shearing interferometry for direct electric field reconstruction (SEA-F-SPIDER) [19].

A part of the uncompressed radiation of the chirped pulse amplification Ti:sapphire laser (central wavelength 800 nm, pulse energy 120 μ J, pulse duration 8 ps, pulse repetition rate 1 kHz) was split from the beam line prior to the laser compressor stage and was focused into the vacuum chamber to create a plasma on the manganese target (Fig. 1). The picosecond heating pulses were focused by a 400 mm focal length lens and created a plasma plume with a diameter of ~ 0.5 mm using an intensity on the target surface of $I_{ps} = 8 \times 10^9$ W cm $^{-2}$.

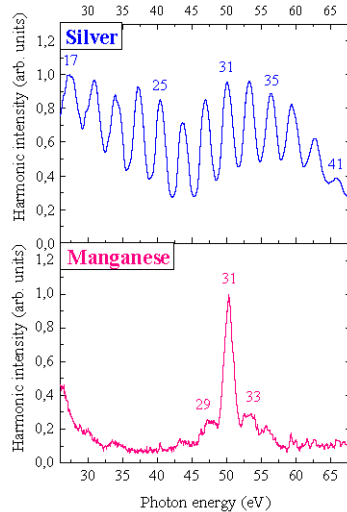


Fig. 2. Harmonic spectra from the silver plasma (upper curve) and manganese plasma (bottom curve).

The femtosecond harmonic drive pulses were focused in a direction orthogonal to that of the heating pulse into the laser plasma using a 400 mm focal length spherical mirror. The delay between plasma initiation and femtosecond pulse propagation was set to 33 ns. The plasma plume and target were translated along the propagation axis of the femtosecond pulse, to analyse the conversion efficiency of harmonic generation at different focusing conditions. The position of the focus of the femtosecond pulse with respect to the plasma area was chosen to maximize the harmonic signal, and the intensity at the plasma area was estimated to be $I_{fs} = 6 \times 10^{14}$ W cm $^{-2}$. The generated harmonics were analysed by a XUV spectrometer consisting of a flat-field grating (1200 lines/mm, Hitachi) and a microchannel plate (Photonis USA, Inc.) coupled to a phosphor screen. The spatially resolved spectra of the generated harmonics were detected by a CCD camera [20].

3. Results and discussion

The harmonic spectrum in the case of the manganese plasma was strikingly different compared with other plasma samples (for example Ag plasma) analysed in separate experiments. While all other samples studied showed a relatively featureless harmonic spectrum with extended cutoff (Fig. 2, upper curve showing the spectrum of harmonics generating in the silver plasma), the Mn plasma allowed the generation of a strong single harmonic substantially enhanced compared with neighbouring ones (Fig. 2, bottom curve).

We note that in earlier work the harmonic spectra from manganese plasmas for 30 fs [13] and 140 fs [14] pulses also showed enhanced harmonics around 50 eV. The assumption of the resonance nature of the enhancement of harmonics of the ~ 800 nm radiation of Ti:sapphire lasers in this spectral region is supported by the presence of a strong giant resonance in the vicinity of 50 eV confirmed by experimental [7,21] and theoretical [22] studies. The enhancement of a single harmonic can be attributed to the broadband resonances of the ions of

few metals, such as V, In, Cd, Cr, Cd, and Mn. These “giant” resonances have been experimentally confirmed in the literature [7,21–23] and discussed recently in a few theoretical studies [24–28].

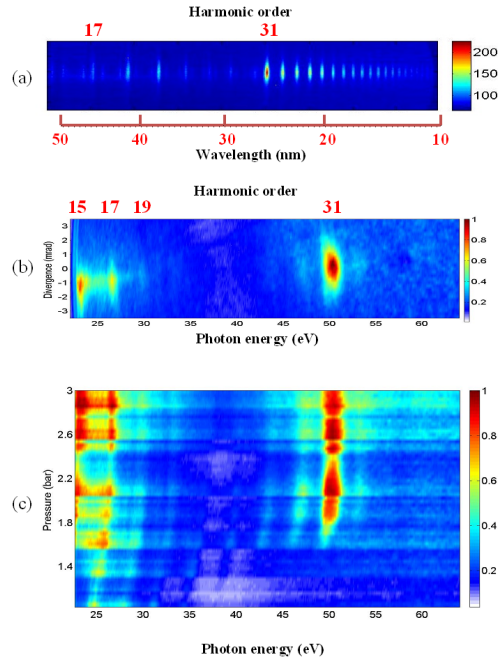


Fig. 3. Raw images of harmonic spectra from manganese plasma in the case of (a) 40 fs and (b) 3.5 fs probe pulses obtained at the same intensity. (c) Raw images of harmonic spectra from Mn plasma at different pressures of neon in the hollow fiber obtained at the same energy of probe laser pulses.

However, in previous studies using multi-cycle drive pulses, the intensity of the enhanced harmonics was only a few times higher than neighboring harmonic orders. We were able to reproduce this behavior in our current experiments using 40 fs pulses from another Ti:sapphire laser (KMLabs, Red Dragon) at similar intensity inside the laser plasma ($4 \times 10^{14} \text{ W cm}^{-2}$). The raw image of the harmonic spectrum presented in Fig. 3(a) shows several enhanced harmonics starting from the 31st order followed by an extended second plateau. The extension of the harmonic cutoff exceeding the 71st order is attributed to the involvement of doubly charged Mn ions as the sources of HHG. This feature of Mn plasma harmonics has already been reported earlier [13]. We also present a typical Mn harmonic spectrum in the case of 3.5 fs pulses (Fig. 3(b)). No second plateau, which was seen in the case of multi-cycle (40 fs) pulses, is observed for the few-cycle pulse. Most strikingly, is the observation of a single very strong, broadband (2.5 eV), 31st harmonic. Only two weak neighboring harmonics (around the strong emission) are seen in the 30–65 eV spectral range. The ratio between the intensities of the enhanced harmonic to the weak neighboring harmonics exceeds one order of magnitude. We note that at a lower intensity of the femtosecond pulse ($< 2 \times 10^{14} \text{ W cm}^{-2}$), the strong harmonic disappeared when using both multi- and few-cycle pulses.

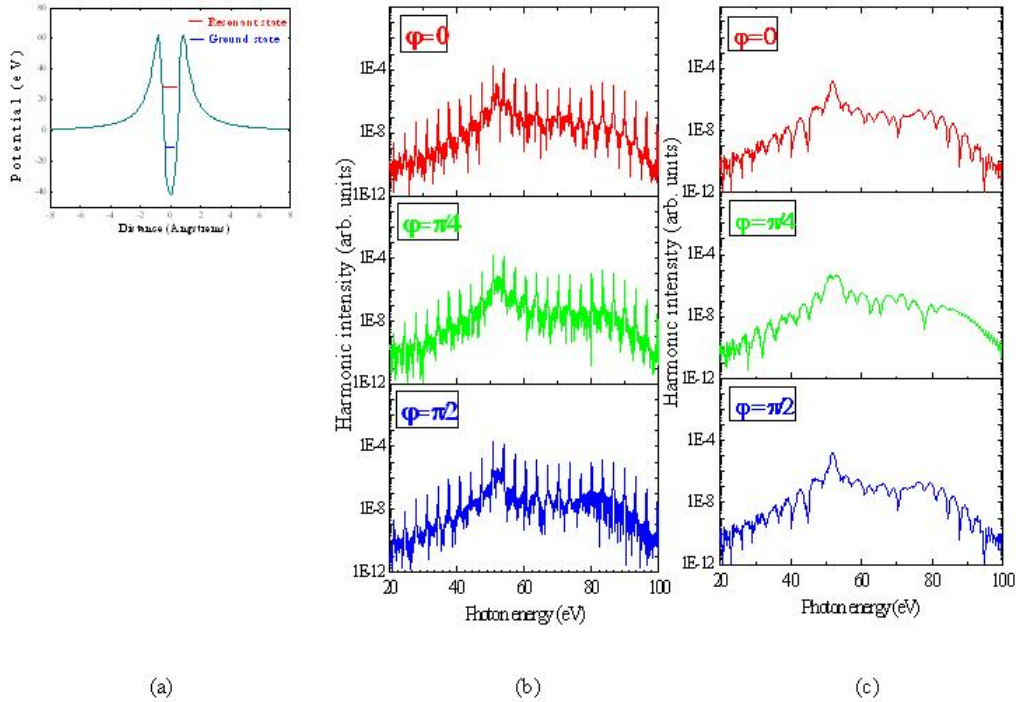


Fig. 4. (a) Potential used for the numerical simulations. (b,c) Calculated HHG spectra using (b) a long (40 fs) pulse and (c) few-cycle pulses at different values of the CEP ($\varphi = 0, \pi/4$, and $\pi/2$).

The distinctive structure of the harmonic spectra, both for 40 fs and 3.5 fs pulses clearly points to the involvement of Mn resonances centred around 50–51 eV. The same can be said about the photoionization or photoabsorption characteristics of Mn^+ plasma, which is due to the ‘giant’ $3p \rightarrow 3d$ resonance [7]. We analysed the laser polarization dependence of this emission and found that the 50 eV radiation abruptly disappears with the change of the polarization state of the femtosecond probe pulses from linear to circular, which is a clear signature of the emission being due to high harmonic generation.

To analyse the effect of the spectro-temporal characteristics of the femtosecond radiation on the harmonic yield, we varied the pressure of neon in the hollow fiber system, thus changing the duration of the harmonic drive pulse [18]. The spectral and intensity variations of manganese harmonic spectra in the range of 22–62 eV as the functions of neon pressure in the hollow fiber are shown in Fig. 3(c). One can clearly see that, with change of pressure (from 1 to 2.3 bar), the single 31st harmonic intensity varies from almost zero to its maximum high value. A blue shift of the harmonics is also evident. Further increase of neon pressure up to 3 bar, at which the experiments with the 3.5 fs pulses were carried out, did not change the harmonic distribution.

In the following we present the results of numerical simulations within a 1D model. We assumed that the main contribution to the resonant peak in the spectrum comes from Mn^+ ions. Note that the ionisation potential of Mn^{2+} ions (33.7 eV) is more than twice higher than the ionisation potential of Mn^+ ions (15.6 eV). We solved the time-dependent Schrödinger equation by means of the split-operator method [29]. The Mn^+ target is modelled using a potential supporting a metastable state by a potential barrier [24,28]. The shape of the potential is (see Fig. 4(a))

$$V(x) = -a + \frac{a}{1 + \exp\left(\frac{x+b}{c}\right)} + \frac{a}{1 + \exp\left(\frac{-x+b}{c}\right)} + \frac{d/(e+x^2)}{1 + \exp\left(\frac{x+b}{c}\right)} + \frac{d/(e+x^2)}{1 + \exp\left(\frac{-x+b}{c}\right)}, \quad (1)$$

where a , b , c , d , and e are parameters. We choose them to be 1.672, 1.16, 0.216, 8.95 and 0.63, respectively, so that the width of the resonance and the energy gap between the ground and the resonant states resemble the experimental data [7]. The metastable state of our model potential is at 51.8 eV above the ground state. The laser field is $E(t) = E_0 f(t) \cos(\omega_0 t + \varphi)$, where $f(t)$ is the pulse envelope, φ denotes the carrier envelope phase (CEP) and ω_0 is the laser frequency corresponding to the central wavelength $\lambda = 760$ nm. The laser intensity is $I_0 = 4 \times 10^{14}$ W cm⁻². A CEP of $\varphi = 0$ means that the maximum of the envelope corresponds to a maximum of $\cos(\omega_0 t)$.

We calculated HHG spectra for pulse shapes with different lengths and for different values of φ (Figs. 4(b) and 4(c)). A \sin^2 envelope with a total length of 4 full cycles was used to model the 3.5 fs pulse, while an envelope with 4 cycles \sin^2 switch-on/off, 13 cycles of constant intensity and 21 cycles total duration was used to model the 40 fs case. The long pulse led to a HHG spectrum that shows well defined peaks at the odd harmonic orders and that is weakly dependent on the CEP (Fig. 4(b)). Figure 4c shows the dependence of the harmonic spectrum on the CEP in the case of the short, few-cycle pulse. In all cases, the resonance dominated the spectrum. The most intense emission occurs around 51 eV, where the metastable state is located. This enhancement has been explained in terms of a four-step model [24], according to which the recombination step is split into two steps: trapping of the returning electron in the metastable state followed by radiative transition into the ground state. An alternative view is that, according to the quantitative rescattering theory [30], the emission spectrum is proportional to the photoionization cross section, which exhibits a peak at the resonance energy. Note that the mechanism is different from the type of harmonic generation described in [31], where the initial state before ionization is already a superposition of ground and excited states. Some difference between harmonic spectra for $\varphi = 0$, $\pi/4$, and $\pi/2$ is found, though we note that the CEP dependence is strongest for the spectrum outside the region of the resonance. For random CEP the substructure of the spectrum will average out as confirmed by numerical averaging over 20 values of the CEP in the range from 0 to π . The shape of resonance peak depends on the CEP, and the case of $\varphi = \pi/4$ appears to be special since a dip due to trajectory interference seems to coincide with the resonance peak.

The experiments described above were carried out without CEP stabilisation (that is, for random CEP values). We also carried out the HHG experiments with Mn plasma using 3.5 fs pulses with stabilized CEP ($\varphi = 0$ and $\pi/2$) and found some differences in that case (Fig. 5), in particular the variation of harmonic distribution observed for the lower order harmonics (compare the middle and bottom curves of Fig. 5; see also our following discussion). The spectral shapes of the 31st harmonic emission were approximately similar for these two fixed values of CEP, while a considerable difference in harmonic spectra was maintained when comparing to longer pulse duration and lower intensity of the driving pulses. Figure 5 shows measurements for 25 fs pulses (upper panel) and 3.5 fs pulses (middle and bottom panels) of the same energy. One can clearly see the absence of harmonic extension and resonance-induced HHG in the case of low-intensity, 25 fs pulses, which has been reported in earlier studies of plasma harmonics from manganese ablation using low intensity pulses [13,14].

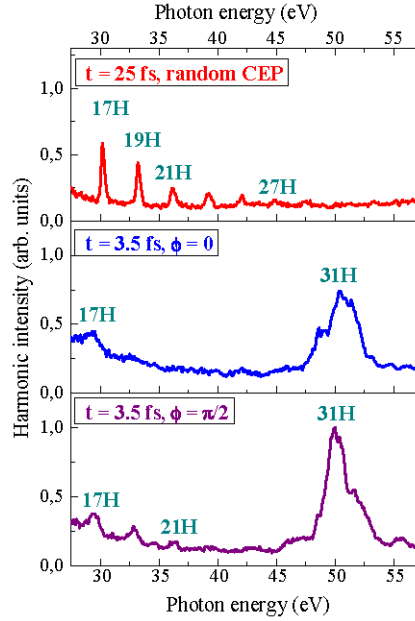


Fig. 5. Experimental harmonic spectra generated from manganese plasma in the case of the absence of gas in the hollow fibre compressor ($t = 25$ fs) and random CEP (upper panel), and at 3 bar pressure ($t = 3.5$ fs) at fixed CEP ($\varphi = 0$, middle panel; $\varphi = \pi/2$, bottom panel).

In order to investigate temporal characteristics of the harmonic emission in our numerical simulations we performed a Gabor transformation [32]:

$$G(\omega, t) = \frac{\int d\tau a(\tau) \exp(i\omega\tau) \exp\left(-\frac{(t-\tau)^2}{2\sigma^2}\right)}{\sqrt{2\pi\sigma^2}}, \quad (2)$$

where $a(\tau)$ is the dipole acceleration from the simulation, σ is a parameter taken to be $\sigma = 1/(3\omega_0)$. The modulus squared, $|G(\omega, t)|^2$, is the time-frequency distribution. The temporal intensity profile of the XUV emission is calculated as the square of the time-dependent dipole acceleration after filtering out the photon energies below 1.2 a.u. (corresponding to 32.7 eV). In fact, the emission profile is not affected much by the filtering since the spectrum is strongly dominated by the resonance. The results are shown in Fig. 6. Comparing the short- and long-pulse regimes, one can notice that, whereas in Figs. 6(b)–6(d) emission of the resonance occurs at the end of the few-cycle pulse, Fig. 6(a) shows that the resonance is repopulated and decaying each half cycle of the multi-cycle pulse. For the short pulse, the emission takes the form of a short burst confined to one or two half cycles of the driving laser field. In our few-cycle pulse for the recollision following the last strong field peak the resonance is only weakly perturbed by the field. Thus the enhanced recombination associated with the resonance is largely confined to this last cycle.

For most CEPs, the emission can be viewed as an isolated sub-fs XUV pulse if the pulse length is defined, in the usual way, as the full width at half maximum. This main emission burst is either preceded or followed by a small side peak. Similar emission profiles are found for three values of the CEP (0, $\pi/4$, and $\pi/2$, Figs. 6(b)–6(d)). The time of maximum emission varies in a range of less than 1 fs with CEP. Our calculations show that we usually get sub-femtosecond XUV pulses or at least ~ 1 femtosecond XUV pulses, for different values of CEP. This is in sharp contrast with the usual strong CEP dependence of isolated attosecond pulse generation [17,33,34]. This suggests that resonance-induced HHG driven by few-cycle

pulses provides a route to isolated XUV attosecond pulse generation with reduced requirements for CEP stabilization.

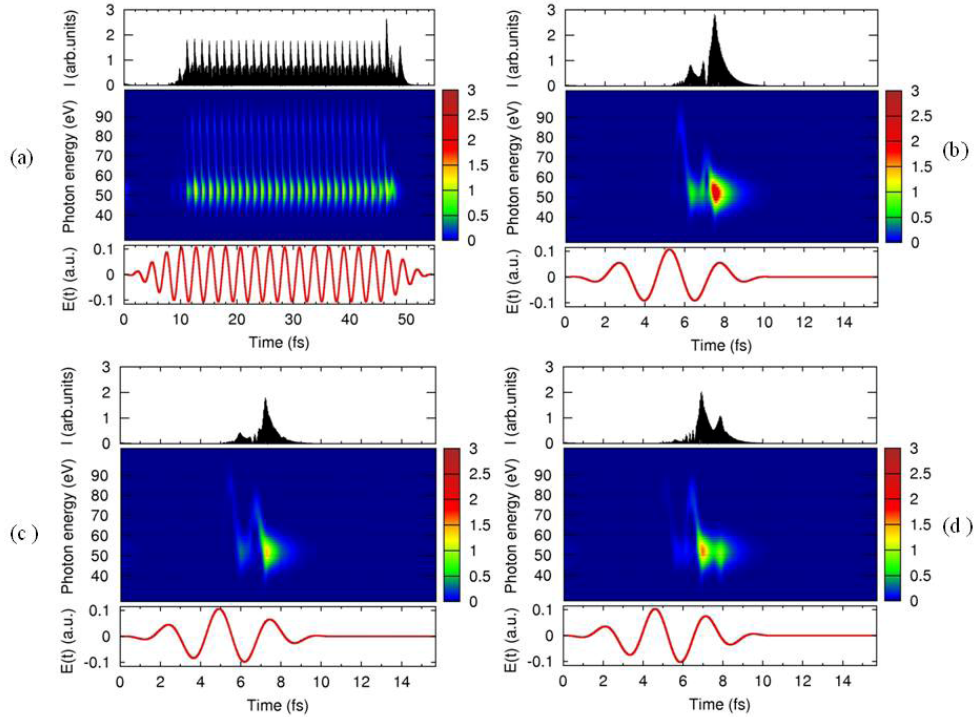


Fig. 6. Calculated results for HHG driven by (a) a long (40 fs) pulse with CEP $\varphi = \pi/4$ and (b-d) few-cycle pulses with CEPs of (b) $\varphi = 0$, (c) $\varphi = \pi/4$, and (d) $\varphi = \pi/2$. The top panels show the HHG temporal intensity profile obtained as the square of the time-dependent dipole acceleration after high pass filtering above 32.7 eV. The middle panels show the time-frequency diagrams. The red curves in the bottom panels show the time dependence of the electric field of the driving laser pulse.

As it was pointed out, our experimental and theoretical studies of harmonic spectra from Mn plasma plumes showed some dependence on the carrier envelope phase of the driving, few-cycle pulses. In Fig. 5 it is evident that, when varying the CEP of the driving 3.5 fs pulse, the 30-40 eV region of the harmonic spectra is changed, with two additional peaks (19th and 21st harmonics) appearing when the CEP varies from 0 to $\pi/2$ rad (middle and bottom panels). The structure of the enhanced spectral windows around the 31st harmonic modifies its shape, the shoulder shifting from the left to the right side of the main peak, and the overall FWHM also decreasing. Some CEP-induced changes in harmonic spectra are also confirmed by the simulations, which point out a different temporal structure of the isolated pulse for various CEP values (Fig. 6). Note that while the shape of the attosecond pulse changes with CEP, the emission time with respect to the IR driving pulse varies little.

The fact that we did not observe a strong CEP dependence of the harmonic spectra in the case of 3.5 fs pulses could be attributed to the presence of a significant density of free electrons in the manganese plasma, which might diminish the difference between the HHG spectra recorded for different values of experimental CEP. The same can be said about other HHG experiments using silver and brass plasmas, which did not show significant differences in harmonic spectra when comparing few-cycle pulses with fixed and random CEP. We also carried out comparative studies with gas media under similar experimental conditions and found a characteristic strong dependence of the HHG spectra on the CEP. Thus the weak influence of the CEP on the harmonic pattern generated by few-cycle pulses from the ablation plumes appears to be a common feature of plasma HHG.

4. Conclusions

In conclusion, we report the observation of harmonic spectra from manganese plasmas driven by 3.5 fs pulses, which are dominated by a single enhanced 31st harmonic at around 50 eV. The spectro-temporal experiments reveal the influence of the drive pulse duration on this process. Analysis of the harmonic energy tuning upon the variation of driving laser pulse duration controlled by change of gas pressure in the hollow fiber compression system show stabilization of the enhanced harmonic's energy and wavelength, which we explain with resonance-induced enhancement at 51 eV. Our theoretical modelling suggests that the emission could constitute an isolated sub-femtosecond pulse. The observed weak CEP dependence might reduce the requirements for CEP stabilisation of the laser. The isolation of a single harmonic order without any filtering could also be useful for various applications where the coherent, short pulse XUV radiation is required, without the losses induced by spectral dispersion or filtering.

Acknowledgments

This research was supported by EPSRC programme (grants No. EP/F034601/1, EP/E028063/1 and EP/I032517/1) as well as European Marie Curie Initial Training Network (Grant No. CA-ITN-214962-FASTQUAST). R. A. Ganeev acknowledges support from the Marie Curie International Incoming Fellowship Grant within the 7th European Community Framework Programme (grant No. 253104). The technical support of P. Ruthven and A. Gregory is gratefully acknowledged.